

A Comprehensive Proteomics Analysis of Urinary Extracellular Vesicles Identifies a Specific Kinase Protein Profile as a Novel Hallmark of Medullary Sponge Kidney Disease



Maurizio Bruschi^{1,7}, Simona Granata^{2,3,7}, Andrea Petretto⁴, Alberto Verlato², Gian Marco Ghiggi⁵, Giovanni Stallone⁶, Giovanni Candiano¹ and Gianluigi Zaza^{2,6}

¹Laboratory of Molecular Nephrology, Istituto di Ricovero e Cura a Carattere Scientifico (IRCCS) Istituto Giannina Gaslini, Genova, Italy; ²Renal Unit, Department of Medicine, University Hospital of Verona, Verona, Italy; ³Department of Medical and Surgical Sciences, University of Foggia, Foggia, Italy; ⁴Core Facilities - Proteomica e Metabolomica Clinica, Istituto di Ricovero e Cura a Carattere Scientifico (IRCCS) Istituto Giannina Gaslini, Genova, Italy; ⁵Division of Nephrology, Dialysis and Transplantation, Istituto di Ricovero e Cura a Carattere Scientifico (IRCCS) Istituto Giannina Gaslini, Genova, Italy; and ⁶Nephrology, Dialysis and Transplantation Unit, University of Foggia, Foggia, Italy

Correspondence: Gianluigi Zaza, Renal Unit, Department of Medicine, University Hospital of Verona, Piazzale A Stefani 1, Verona 37126, Italy. E-mail: gianluigi.zaza@univr.it

⁷MB and SG contributed equally to the study.

Received 21 December 2021; revised 17 February 2022; accepted 21 February 2022; published online 2 March 2022

Kidney Int Rep (2022) 7, 1420–1423; <https://doi.org/10.1016/j.ekir.2022.02.015>

KEYWORDS: extracellular vesicles; idiopathic calcium nephrolithiasis; medullary sponge kidney; proteomics

© 2022 International Society of Nephrology. Published by Elsevier Inc. This is an open access article under the CC BY-NC-ND license (<http://creativecommons.org/licenses/by-nc-nd/4.0/>).

INTRODUCTION

Recent advances in the high-throughput technologies and data analysis have led to better understanding of the biological processes involved in several kidney disorders,^{1,S1,S2} including the medullary sponge kidney (MSK) disease, a rare congenital malformation characterized by dilation of the collecting ducts in the renal papillae, urinary acidification and concentration defects, cystic anomalies of precalyceal ducts associated with a high risk of nephrocalcinosis, and recurrent kidney stones.²

Our research group, analyzing both the whole urinary proteome profile^{3,4} and the protein content of urinary extracellular vesicles (microvesicles and exosomes),^{5,6} has previously identified specific biological fingerprints of MSK able to discriminate this disorder from other clinical conditions including idiopathic calcium nephrolithiasis (ICN)³ and selected potential biomarkers that could allow earlier diagnosis of MSK avoiding expensive and invasive diagnostic approaches.

Laminin subunit alpha 2 was one of the promising identified proteins. This is a major component of the extracellular matrix that may have a role in cystic dilatation of the precalyceal ducts and in renal tubular epithelial cell polarization.^{S3,S4}

Instead, the proteomic analysis of urinary extracellular vesicles^{S5,S6} was able to differentiate patients with MSK from those affected by autosomal dominant polycystic kidney disease.⁶ Analysis of the protein content of urinary extracellular vesicles of patients with the 2 disorders suggested a different mechanism of cystogenesis and probably confirmed earlier reports indicating MSK could be an inborn malformation.^{S7}

However, even with the reports of these literature, the physiopathologic mechanism associated with this disease is not fully understood. Therefore, we reinterrogated proteomic raw data previously obtained from urinary microvesicles of MSK and ICN⁵ applying updated bioinformatic methodologies to identify a specific urinary extracellular vesicle proteomic fingerprint differentiating patients with MSK from those affected by ICN (controls).

RESULTS

The protein composition of urinary exosomes and microvesicles of patients with MSK and ICN was determined by mass spectrometry (details in the [Supplementary Methods](#)). We identified 2978 proteins in the exosomes and microvesicles isolated from urine of patients with MSK and ICN ([Supplementary](#)

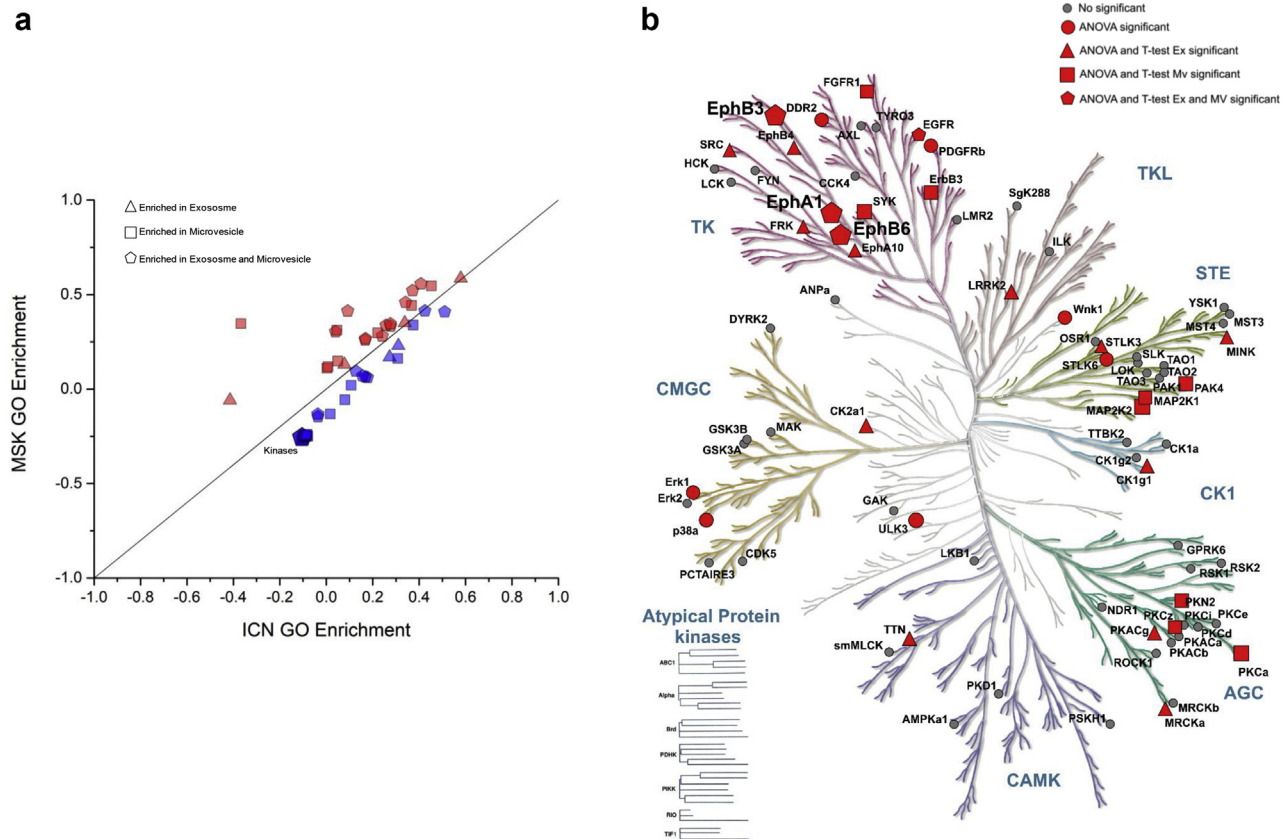


Figure 1. GO annotation enrichment analysis of the total proteins identified and kinome tree of exosomes and microvesicles isolated from urine of MSK and ICN samples. (a) Dot plot shows the enriched signatures in exosomes, microvesicles isolated from urine of patients with MSK and ICN. In the graph, the points located on the straight line passing through the coordinates (1x, 1y) and (-1x, -1y) are the equally enriched signatures, whereas those above or under this line are positively enriched in MSK or ICN samples, respectively. The triangle, square, and pentagon points indicate the GO annotation enriched in the exosomes, microvesicles, or both the extracellular vesicles of the MSK or ICN samples, respectively. Exosomes and microvesicles of the ICN samples are enriched in kinases (see [Supplementary Table S3](#)). (b) Kinome tree showing the statistical significance of identified kinases. Gray circles indicate the nonsignificant proteins, whereas red circles, triangles, squares, and pentagons indicate the most statistically significant kinases in analysis of variance (ANOVA), ANOVA, and *t* test for exosomes, ANOVA and *t* test for microvesicles, and ANOVA and *t* test for exosomes and microvesicles, respectively (see [Supplementary Table S4](#)). ANOVA, analysis of variance; GO, gene ontology; ICN, idiopathic calcium nephrolithiasis; MSK, medullary sponge kidney.

[Tables S1](#) and [S2](#)). Among these, 2491, 2456, 2471, and 2190 were classified in the exosomes or microvesicles of MSK or ICN samples, respectively. In addition, 1774 proteins (60.5%) overlapped in all samples, whereas only 119 (4.1%) and 25 (0.9%) were exclusive for exosomes and microvesicles of MSK samples and 57 (1.9%) and 83 (2.8%) were exclusive for exosomes and microvesicles of ICN samples, respectively ([Supplementary Figure S1](#)).

Total identified proteins were classified according to the cellular component, molecular function and biological process of the gene ontology signatures. Using these classification and other gene ontology annotations extracted from UniProt database (www.uniprot.org),⁵⁸ a gene ontology enrichment analysis was performed.

This analysis showed an enrichment of 57 signatures ([Supplementary Table S3](#)). Interestingly, the most discriminative signature in the extracellular vesicles

able to differentiate the 2 study groups was that including kinases ($n = 82$ identified proteins) ([Figure 1a](#) and [Supplementary Table S3](#)). Among the 82 identified kinases, 62, 47, 68, and 71 were identified in the exosomes or microvesicles of the MSK or ICN samples, respectively.

Noteworthy, 37 of 82 kinases (45.1%) overlapped in all samples, whereas only 2 of 82 (2.4%), 0 of 82 (0%), 5 of 82 (6.1%), and 4 of 82 (4.9%) were exclusive for the exosomes or microvesicles of the MSK or ICN samples, respectively ([Supplementary Figure S2A](#)). Moreover, 34 of 82, 17 of 82, and 14 of 82 were highlighted in analysis of variance test and *t* test in the comparison of exosomes or microvesicles of MSK and ICN, respectively ([Supplementary Figure S2B](#) and [Supplementary Table S4](#)).

Identified kinases in the exosomes or microvesicles of the MSK or ICN samples were visualized by means of the interactive web application CoralTree⁵⁹ ([Figure 1b](#)

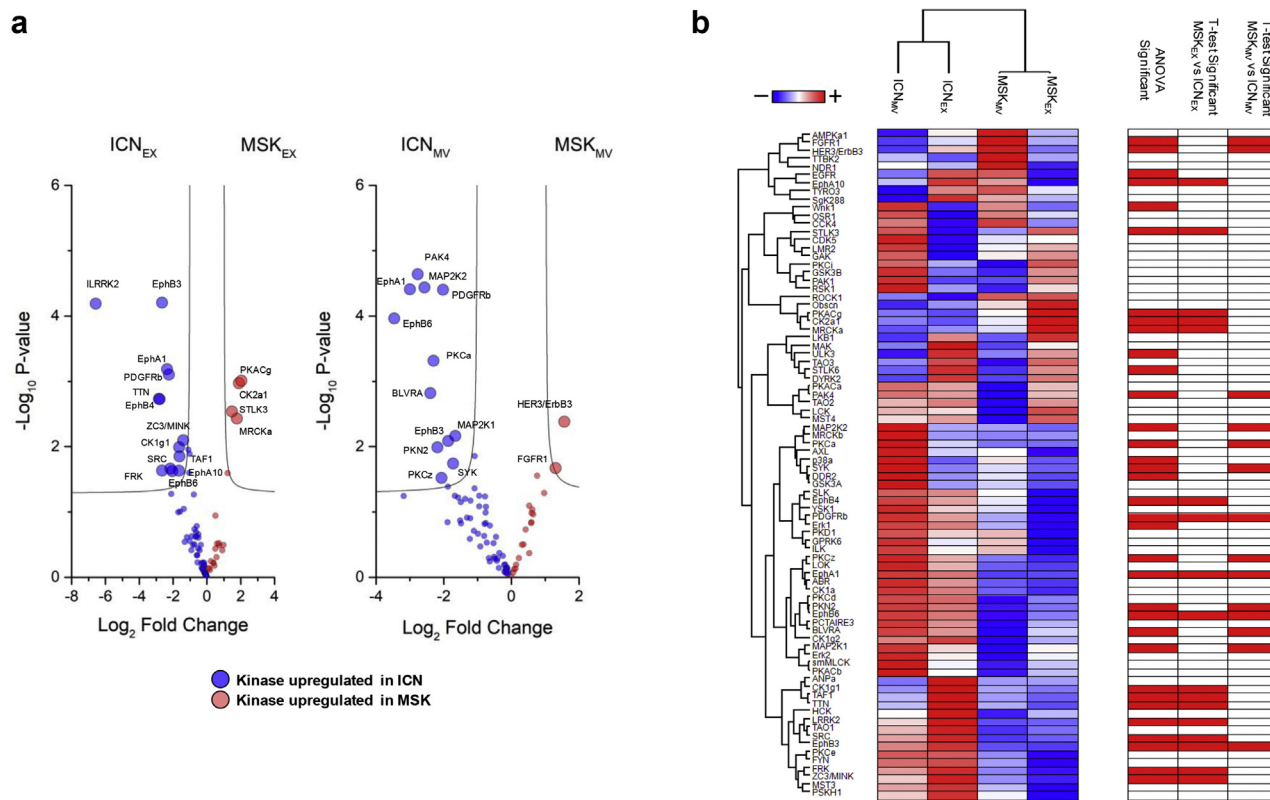


Figure 2. Volcano plots and heatmap of kinases of exosomes and microvesicles from urine of patients with MSK and ICN. (a) Volcano plot of total identified kinases in exosomes and microvesicles from urine of MSK and ICN samples. Small and large blue or red circles indicate the nonsignificant and significant kinases upregulated in ICN or MSK samples, respectively. Black line indicates the limits of statistical significance. (b) Heatmap of total kinases identified. Heatmap of profiles of 82 kinases (see [Supplementary Table S4](#) for detail). Each row represents a kinase and each column a type of samples. Normalized Z-scores of kinase abundance are depicted by a pseudocolor scale (red, white, and blue indicate positive equal and negative expression, respectively) compared with each kinase value. The dendrogram displays unsupervised hierarchical clustering analysis, where similar sample/kinase profile values are next to each other. Visual inspection of the dendrogram and heatmap demonstrates the ability of the kinases to discriminate between exosomes and microvesicles of MSK and ICN samples. ICN, idiopathic calcium nephrolithiasis; MSK, medullary sponge kidney.

and [Supplementary Figures S3 and S4](#)) and volcano plot ([Figure 2a](#) and [Supplementary Tables S3 and S4](#)).

The expression profile of these proteins in the exosomes and microvesicles of the MSK and ICN samples, after Z-score normalization, was visualized in a heatmap diagram ([Figure 2b](#)).

Finally, according to several statistical algorithms, ephrin receptors (EphA1, EphB3, and EphB6) resulted the most promising kinase biomarkers for differentiating the 2 study groups ([Figure 2b](#)). Enzyme-linked immunosorbent assay (ELISA) validated these results ([Supplementary Figure S5](#)).

DISCUSSION

In this study bioinformatic analysis revealed that several kinases were able to differentiate MSK from ICN (control) and that 3 ephrin receptors (EphA1, EphB3, and EphB6) resulted the most significantly down-regulated proteins in MSK versus ICN.

Ephrin receptors, belonging to the largest subfamily of receptor tyrosine kinases, are subdivided based on

sequence similarity into an A subclass (EphA1–EphA8) and a B subclass (EphB1–EphB4, EphB6). Their ligands, the ephrins, are cell surface-bound proteins classified into 2 subfamilies based on their mode of membrane attachment: ephrins A (A1–A6) and ephrins B (B1–B3).^{S10}

Ephrin receptors and ephrins are expressed in almost all tissues of a developing embryo and are involved in a wide array of developmental processes (including cardiovascular and skeletal development, axon guidance, modulation of cell adhesion and migration).^{S11}

These biological processes, whether deregulated, may be involved in the pathophysiology of the MSK disease. In fact, based on available literature, MSK could belong to congenital anomalies of the kidney and urinary tract.^{2,S12,S13} Its association with several developmental defects in other organs² suggests that this defective embryogenic step could be shared by the various organs involved.^{S14–S16}

In addition, as recently reported,⁷ tyrosine kinases and ephrin ligands may regulate kidney cytoarchitecture once development is completed. Immunolocalization

experiments revealed that EphB2 is localized in the tubules of the inner and outer medulla and EphB6 is in the tubules of the outer medulla and cortex. By contrast, EphB1 was detected in the tubules throughout the whole nephron.^{7,S17}

More recently, it has been shown that EphB2 has no role in kidney development but is abnormally activated after kidney injury contributing to renal fibrosis.⁸ The down-regulation of ephrins in MSK may, therefore, represent a potential biological protective mechanism to prevent the fibrosis. We cannot also exclude that the higher levels of ephrins in ICN may be in part caused by a calcification-induced tissue microinflammation and proinflammatory macrophage accumulation.^{S18}

EphB signaling by RhoA activation and Rac1 inactivation induces cell retraction, enlargement of focal adhesions, and prominent stress fibers in primary cultures of medullary tubule cells. These results suggest that EphB receptor signaling through Rho family GTPases regulates the cytoarchitecture and spatial organization of the tubule cells in the adult kidney medulla and, therefore, may affect the reabsorption ability of the kidney.^{S19} Moreover, Rho family GTPases regulate cystogenesis⁹ and correct cellular polarization^{S20}; therefore, down-regulation of EphB signaling in MSK could play a role in cystic dilations of the distal tubules and in altered polarization of the renal tubular cells, which characterize these patients.^{S16}

The results of this study (and our previous findings) demonstrated that a complex biological machinery is deregulated in MSK. Several biological elements including laminins (mainly laminin 2) together with ephrins (in particular, EphB3 and EphB6) and other kinases (e.g., MAPK) could orchestrate cell proliferation, cystic dilations of precalyceal ducts, and extracellular matrix remodeling typically associated with this disease.

Because 8% of patients with MSK in Italy have mutations in GDNF gene,^{S21} we cannot exclude that the GDNF/RET deregulation may influence kinase expression.

Although additional studies are necessary to define the impact of kinases and ephrin signaling in MSK, we can postulate that kinase down-regulation could be a characteristic of this pathology and represent a new and previously unrecognized biological mechanism associated with this rare kidney disorder. Finally, the selected proteins (mainly EphA1, EphB3, and EphB6) may represent future disease biomarker and potential therapeutic targets.

DISCLOSURE

All the authors declared no competing interests.

SUPPLEMENTARY MATERIAL

Supplementary File (PDF)

Supplementary Methods.

Supplementary References.

Figure S1. Venn diagram of total proteins identified and gene ontology annotation enrichment analysis.

Figure S2. Venn diagram of total kinases identified and Venn diagram of statistically significant proteins.

Figure S3. Kinome tree of exosomes isolated from urine of MSK and ICN samples.

Figure S4. Kinome tree of microvesicles isolated from urine of MSK and ICN samples.

Figure S5. ELISA validated proteomic data.

Table S1. List of total protein identified in exosomes and microvesicles isolated from urine of MSK and ICN patients.

Table S2. List of total proteins identified in exosomes and microvesicles isolated from urine of MSK and ICN patients with their statistics.

Table S3. Gene Ontology enrichment in exosomes and microvesicles isolated from urine of MSK and ICN patients.

Table S4. List of total kinases identified in exosomes and microvesicles isolated from urine of MSK and ICN patients.

REFERENCES

1. Rhee EP. How omics data can be used in nephrology. *Am J Kidney Dis.* 2018;72:129–135. <https://doi.org/10.1053/j.ajkd.2017.12.008>
2. Fabris A, Anglani F, Lupo A, Gambaro G. Medullary sponge kidney: state of the art. *Nephrol Dial Transplant.* 2013;28:1111–1119. <https://doi.org/10.1093/ndt/gfs505>
3. Fabris A, Bruschi M, Santucci L, et al. Proteomic-based research strategy identified laminin subunit alpha 2 as a potential urinary-specific biomarker for the medullary sponge kidney disease. *Kidney Int.* 2017;91:459–468. <https://doi.org/10.1016/j.kint.2016.09.035>
4. Granata S, Bruschi M, Deiana M, et al. Sphingomyelin and medullary sponge kidney disease: a biological link identified by omics approach. *Front Med (Lausanne).* 2021;8:671798. <https://doi.org/10.3389/fmed.2021.671798>
5. Bruschi M, Granata S, Candiano G, et al. Proteomic analysis of urinary extracellular vesicles reveals a role for the complement system in medullary sponge kidney disease. *Int J Mol Sci.* 2019;20:5517. <https://doi.org/10.3390/ijms20215517>
6. Bruschi M, Granata S, Santucci L, et al. Proteomic analysis of urinary microvesicles and exosomes in medullary sponge kidney disease and autosomal dominant polycystic kidney disease. *Clin J Am Soc Nephrol.* 2019;14:834–843. <https://doi.org/10.2215/CJN.12191018>
7. Weiss AC, Kispert A. Eph/ephrin signaling in the kidney and lower urinary tract. *Pediatr Nephrol.* 2016;31:359–371. <https://doi.org/10.1007/s00467-015-3112-8>
8. Huang Z, Liu S, Tang A, et al. Key role for EphB2 receptor in kidney fibrosis. *Clin Sci (Lond).* 2021;135:2127–2142. <https://doi.org/10.1042/CS20210644>
9. Rogers KK, Jou TS, Guo W, Lipschutz JH. The Rho family of small GTPases is involved in epithelial cystogenesis and tubulogenesis. *Kidney Int.* 2003;63:1632–1644. <https://doi.org/10.1046/j.1523-1755.2003.00902.x>